Available online at www.sciencedirect.com
ScienceDirect
Journal of Nuclear Materials 367–370 (2007) 1018–1022
journal of nuclear materials
www.elsevier.com/locate/jnucmat

Compatibility between Be–Ti alloys and F82H steel

K. Tsuchiya [a,*], H. Kawamura [b], T. Ishida [b]

[a] Directorates of Fusion Energy Research, Japan Atomic Energy Agency (JAEA), 4002, Oarai-machi, Higashi-ibaraki-gun, Ibaraki 311-1393, Japan
[b] Neutron Irradiation and Testing Reactor Center, Japan Atomic Energy Agency (JAEA), 4002, Oarai-machi, Higashi-ibaraki-gun, Ibaraki 311-1393, Japan

Abstract

Beryllium (Be) metal is a reference material for a neutron multiplier in the fusion blanket design. However, Be metal may have problems such as high reactivity and large swelling at high temperature and high neutron dose in the DEMO fusion blanket. Beryllium alloys such as Be–Ti are promising candidates for advanced neutron multipliers from the viewpoints of high melting point, high beryllium content, low radio-activation, and good chemical stability. In this study, the compatibility between Be–Ti alloys that include αBe phase and the structural material F82H was investigated. The reaction product of Be_2Fe was analyzed by X-ray diffraction on the surface of F82H after compatibility testing. The thickness of the reaction layer for the Be–5at.%Ti and Be–7at.%Ti specimens was almost the same. And the thickness for these alloys tested at 800 °C for 1000 h was less than 50 μm, which is much smaller than the previously obtained value, ~200 μm, for Be under the same conditions.

1. Introduction

Beryllium (Be) metal is a reference material as a neutron multiplier in the fusion blanket design [1,2]. However, it may not be applicable to a DEMO blanket that requires high temperature (~900 °C) and high neutron dose (~50 dpa, ~20 000 appm He) because of high reactivity and large swelling under these conditions. However, beryllium alloys such as Be–Ti and Be–V are promising candidates for advanced neutron multipliers from the viewpoints of high melting point, high beryllium content, low activation, good chemical stability, etc. [3–5].

In previous papers, compatibility of Be and Be–Ti alloys with SS316LN was evaluated [6,7]. The thickness of the reaction layer between Be–Ti and SS316LN was smaller than that between Be and SS 316LN. However, compatibility of Be–Ti alloys with F82H that is a candidate structural material for fusion reactor has not been evaluated.

In the present study, the compatibility between Be–Ti alloys and F82H was investigated. Three kinds of Be–Ti specimens (Be–3at.%Ti, Be–5at.%Ti and Be–7at.%Ti) were prepared, and these Be–Ti alloys with αBe phase, which has better ductility than stoichiometric $Be_{12}Ti$, were tested.

* Corresponding author. Tel.: +81 29 266 7369; fax: +81 29 266 7481.
E-mail address: tsuchiya.kunihiko@jaea.go.jp (K. Tsuchiya).

0022-3115/$ - see front matter © 2007 Elsevier B.V. All rights reserved.
doi:10.1016/j.jnucmat.2007.03.186

2. Experimental

2.1. Specimens

Be–Ti specimens with three levels of titanium (Be–3at.%Ti, Be–5at.%Ti and Be–7at.%Ti) were fabricated from beryllium and titanium powder by an arc melting process. The specimens were machined to disks which were approximately 8 mm in diameter and 2 mm in thickness, and then mirror-polished on the surface. These Be–Ti specimens were prepared by NGK Insulators, Ltd. The chemical compositions of the Be–Ti specimens are shown in Table 1. The content of BeO was calculated from Be content in residual after dissolution of Be–Ti specimen, and it was 0.27 wt% at maximum. The surface of the Be–Ti specimens was ultrasonically cleaned with acetone. Fig. 1 shows the microstructures of the Be–3at.%Ti, Be–5at.%Ti and Be–7at.%Ti specimens. This figure also shows microstructures of hot-pressed high purity beryllium (S65C) for comparison. The amount of the Be phase in the specimens decreases with increasing the Ti content.

F82H steel, which is a typical candidate structural material for fusion reactors, was evaluated for its compatibility with the Be–Ti alloys in this experiment. The chemical composition of the F82H specimens is shown in Table 1. The specimen dimension was 10 mm in diameter and 2 mm in

Table 1
Chemical compositions of the specimens

Material (wt%)	Elements							
	Be	Ti	BeO	Mg	Al	Si	Fe	Co
Be–3at.%Ti	85.3	14.3	0.23	<0.001	0.075	0.049	0.036	<0.001
Be–5at.%Ti	78.4	21.3	0.26	0.002	0.057	0.035	0.036	<0.001
Be–7at.%Ti	71.0	28.7	0.27	0.001	0.053	0.031	0.026	<0.001
	Fe	Cr	Ni	W	Mn	Al	V	C
F82H	Bal.	7.78	0.02	1.98	0.1	0.001	0.07	0.09

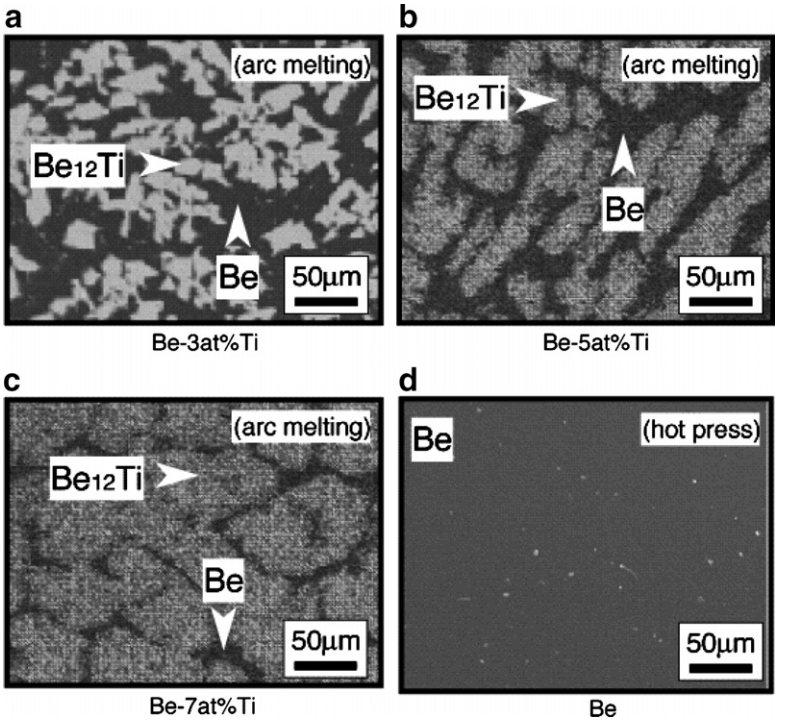

Fig. 1. Microstructures of Be–Ti alloys before the compatibility tests, together with that of Be for comparison.

thickness. The F82H specimens were also mirror-polished and ultrasonically cleaned with acetone.

2.2. Procedure for compatibility tests

The configuration and preparation of the capsule for compatibility tests were described in the previous paper [7]. Diffusion couples for the compatibility tests consisted of Be–3at.%Ti/F82H, Be–5at.%Ti/F82H or Be–7at.%Ti/F82H. Compatibility tests were carried out at 600, 700 and 800 °C by heating the diffusion couples in an electric furnace under vacuum conditions for times of 100, 300 and 1000 h. After heating interactions between the materials were analyzed as follows.

The contacting surface of each specimen was observed by optical microscopy, and X-ray diffractometry (XRD) was performed to identify the reaction products in the near surface region. The microstructure and thickness of the reaction layer were analyzed in the cross section by scanning electron microscopy (SEM). The composition of the layer was identified by electron probe microanalysis (EPMA).

3. Results and discussion

3.1. Identification of reaction products

After testing, evidence of chemical interaction was investigated visually. It was observed that the reaction areas of the contacting surfaces of Be–3at.%Ti/F82H, Be–5at.%Ti/F82H and Be–7at.%Ti/F82H increased with increasing temperature and time.

XRD patterns on the surface of each Be–Ti alloy and F82H for different testing conditions were almost the same. Results of XRD at the Be–5at.%Ti alloy and F82H surfaces at 600 and 800 °C after 1000 h are shown in Fig. 2. On the Be–Ti specimen side, no reaction products were found by XRD at 600 or 800 °C. On the other hand, reaction products were observed on the F82H side by XRD. Be_2Fe was identified as a reaction product on the surface of the F82H in contact with each Be–Ti specimen.

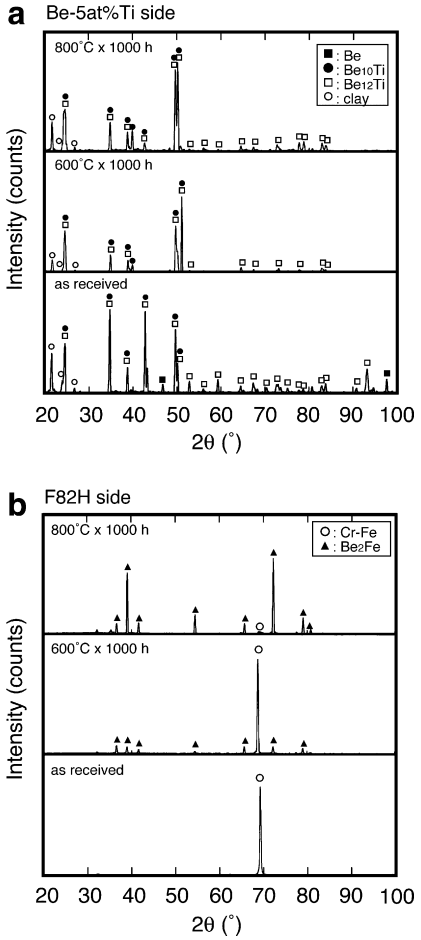

Fig. 2. XRD profiles on the surface of Be–5at.%Ti alloy and F82H after the compatibility tests.

3.2. SEM/EPMA analyses of specimens

Reaction layers were not found on any of the Be–Ti alloy surfaces by SEM observation after testing at 600 and 700 °C. However, a deficiency of Be was observed after testing at 800 °C. On each F82H side, only a thin layer was found at 600 °C. On the other hand, one surface reaction layer and one subsurface diffusion layer were observed on each F82H surface of the Be–Ti couples after testing at 700 and 800 °C, as shown in Fig. 3. Observation of these reaction and diffusion layers on the structural material side was reported by Flament et al. [8] after compatibility tests of beryllium with SS316L or two martensitic steels (1.4914 and HT9).

Quantitative point analyses on each F82H side were performed by EPMA for the typical phases observed by SEM. Fig. 3 shows results of the analysis on the reaction and diffusion layers. Thickness of the reaction layer (region A in Fig. 3) of Be–5at.%Ti/F82H and Be–7at.%Ti/F82H was about 45 and 35 μm, respectively. The contents of Be

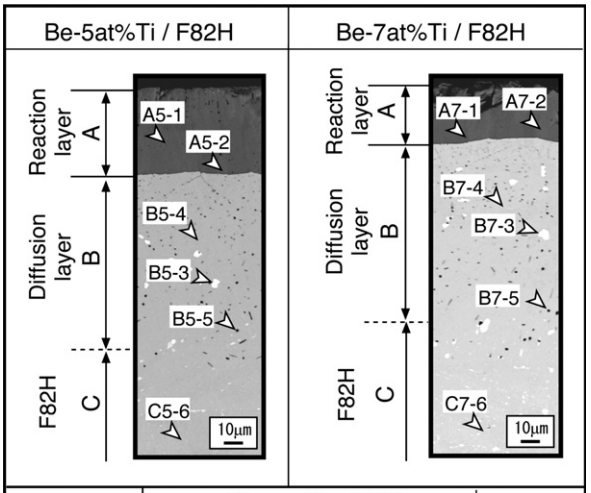

Measuring point		Composition (at%)					Estimated compound
		Be	Ti	Fe	Cr	W	
A Dark Gray	A5-1	71.9	0.0	25.4	2.3	0.4	Be_2Fe
	A7-1	72.6	0.0	24.7	2.2	0.4	
A Light Gray	A5-2	71.2	0.0	26.1	2.4	0.4	Be_2Fe
	A7-2	70.4	0.0	26.6	2.5	0.5	
B White	B5-3	15.5	0.0	66.4	6.7	11.4	Fe-Cr (Be_2Fe) (Fe-W)
	B7-3	17.4	0.0	62.4	6.0	14.2	
B Gray	B5-4	10.3	0.0	81.7	7.7	0.2	Fe-Cr Be_2Fe
	B7-4	8.9	0.0	82.8	8.0	0.2	
B Black	B5-5	24.4	0.0	69.0	6.4	0.2	Be_2Fe (Fe-Cr)
	B7-5	21.7	0.0	71.6	6.6	0.2	
C Gray	C5-6	0.0	0.0	91.0	8.4	0.6	Fe-Cr
	C7-6	0.0	0.0	91.2	8.2	0.6	

Fig. 3. Result of quantitative EPMA analyses of two layers of Be–5at.%Ti/F82H and Be–7at.%Ti/F82H (testing condition: 800 °C × 1000 h).

and Fe in the reaction layer (A) were about 71 and 25 at.%, respectively. It is considered that the phase in the reaction layer was Be_2Fe. Thickness of the diffusion layer (region B in Fig. 3) in couples with both Be–5at.%Ti/F82H and Be–7at.%Ti/F82H was about 100 μm. Three phases existed in the diffusion layer; gray phases and white phases in the diffusion layer (B) were supposed to be Fe–Cr and Fe–W phases, respectively. It is considered that small black particles were a mixture of Be, Be_2Fe and Fe–Cr phases. In the region C (F82H) in Fig. 3, the contents of Fe and Cr were almost the same as those in F82H. Titanium was not detected in the reaction layer nor in the F82H base metal.

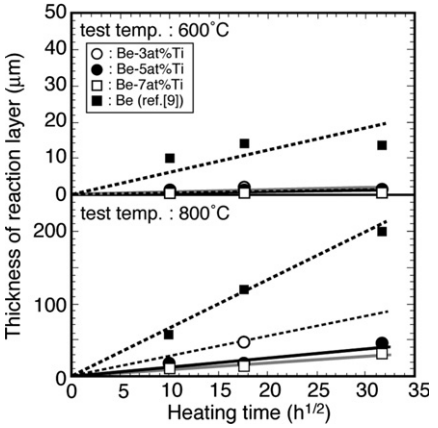

Fig. 4. Change in thickness of the reaction layer with test time.

3.3. Thickness and growth rate of reaction layer

Fig. 4 shows results of thickness measurements of the reaction layer. The thickness of the reaction layer between Be–Ti alloys and F82H after testing at 600 °C for 1000 h was less than 3 μm, whereas the reaction layer with beryllium metal was about 15 μm thick [9]. At 800 °C for 1000 h, the thickness of the reaction layer of Be–5at.%Ti and Be–7at.%Ti was less than 50 μm, whereas that of beryllium metal was about 200 μm [9]. It is obvious that the interaction between Be–Ti alloy and F82H was much less than that between Be and F82H.

Fig. 5 shows the relationship between the content of titanium and the thickness of the reaction layer using the results of the present study and Ref. [9]. The thickness of the reaction layer decreases with

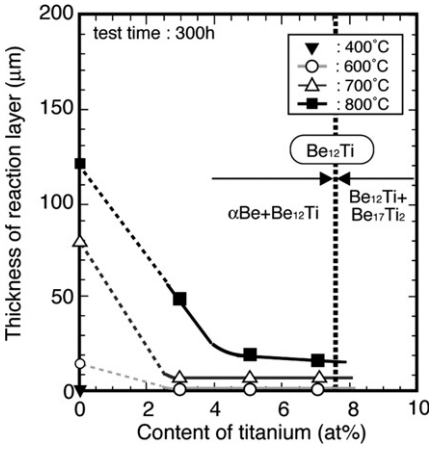

Fig. 5. Relationship between content of titanium in Be–Ti alloys and thickness of reaction layer.

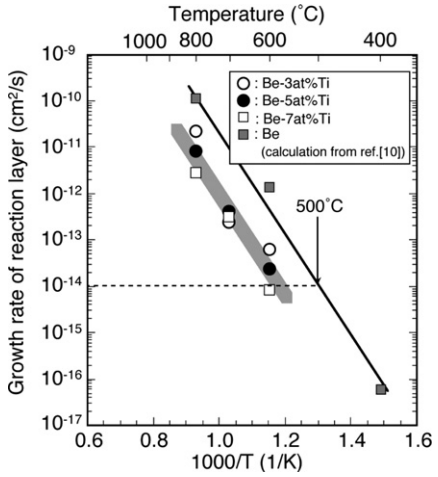

Fig. 6. Growth rate of reaction layer as a function of the reciprocal temperature.

increasing the content of Ti in Be–Ti alloys. It is considered that $Be_{12}Ti$ is less chemically reactive with F82H and that the amount of $Be_{12}Ti$ in Be–Ti alloys increases with increasing the Ti content up to a Ti content of 7 at.%.

The growth rate of the reaction layer evaluated as in Ref. [10] is shown in Fig. 6 as a function of the reciprocal temperature. The growth rate in Be–Ti alloys in the present study was smaller than that of Be, and it decreased with increasing the Ti content in the Be–Ti alloy. The maximum temperature of Be for use in the fusion blanket is assessed to be 500 °C, taking into account the swelling limitation [11]. The growth rate of Be is estimated to be 1×10^{-14} cm^2/s at 500 °C (see in Fig. 6), and it is considered that the maximum utilization temperature of the Be–Ti alloys is about 600 °C.

4. Conclusions

The compatibility between Be–Ti alloys (Ti content: 3–7 at.%) and F82H has been studied. The Be–Ti alloys showed some advantages over Be, and the following conclusions can be made:

(1) Reaction and diffusion layers were observed on the F82H side after compatibility tests of Be–Ti alloys and F82H. The thickness of the reaction layer was smaller than that between Be and F82H after testing at 700 and 800 °C. On the other hand, surface deficiency in Be was observed but reaction layers were not observed on the Be–Ti alloy side.

(2) The gray phase in the reaction layer on the F82H side was composed of Be_2Fe, and the thickness of the gray phase decreased with increasing the content of Ti.

(3) Good compatibility between Be–Ti alloy and F82H was clearly observed, and it was suggested that the Be–Ti alloys (Ti content: 3–7 at.%) could be used up to about 600 °C as far as their compatibility with F82H is concerned.

References

[1] H. Kawamura, M. Okamoto (Eds.), in: Proceedings of the Third IEA International Workshop on Beryllium Technology for Fusion, October 22–24, Mito, Japan, JAERI-Conf 98-001, 1997.
[2] F. Scaffidi-Argentina, G.R. Longhurst, V. Shestakov, H. Kawamura, Fus. Eng. Des. 51&52 (2000) 23.
[3] H. Kawamura, H. Takahashi, N. Yoshida, V. Shestakov, Y. Ito, M. Uchida, H. Yamada, M. Nakamichi, E. Ishitsuka, Fus. Eng. Des. 61&62 (2002) 391.
[4] H. Kawamura, E. Ishitsuka, K. Tsuchiya, M. Nakamichi, M. Uchida, H. Yamada, K. Nakamura, H. Ito, T. Nakazawa, H. Takahashi, S. Tanaka, N. Yoshida, S. Kato, Y. Ito, Nucl. Fusion 43 (2003) 675.
[5] H. Kawamura, H. Takahashi, N. Yoshida, Y. Mishima, K. Ishida, T. Iwadachi, A. Cardella, J.G. van der Laan, M. Uchida, K. Munakata, Y. Sato, V. Shestakov, S. Tanaka, J. Nucl. Mater. 329–333 (2004) 112.
[6] H. Kawamura, M. Uchida, V. Shestakov, J. Nucl. Mater. 307–311 (2002) 638.
[7] K. Tsuchiya, M. Uchida, H. Kawamura, Fus. Eng. Des. 81 (2006) 1057.
[8] T. Flament, P. Fauvet, J. Sannier, J. Nucl. Mater. 155–157 (1988) 496.
[9] H. Kawamura, M. Kato, E. Ishitsuka, S. Hamada, K. Nishida, M. Saito, Fus. Eng. Des. 29 (1995) 475.
[10] V. McGahay, J. Non-Cryst. Solids 349 (2004) 234.
[11] M.C. Billone, C.C. Lin, D.L. Baldwin, Fus. Technol. 19 (1991) 1707.